An Analysis of a Broad-Band Coaxial Hybrid Ring*

V. J. ALBANESE† AND W. P. PEYSER‡

Summary—This paper describes a broad-band coaxial hybrid ring which has excellent isolation and balance characteristics. The ring differs from the conventional hybrid in that the fourth arm has a series-type balun feed and is positioned so that a plane of symmetry exists through two of the arms. Isolation between these arms and balance between the output arms are theoretically independent of frequency. The admittance and VSWR of the input arms are computed by bisecting the ring about the plane of symmetry and employing standard Smith Chart techniques. Corresponding experimental data are included. A comparison is made with the conventional coaxial hybrid ring.

Coaxial Hybrid Symmetric About Arms 1 and 4

THE symmetric coaxial hybrid ring (Fig. 1) was first presented schematically by Tyrell as one of the six fundamental forms.[1] It differs from the conventional hybrid (Fig. 2) in the positioning and type of feed at arm 4. In the conventional coaxial hybrid all arms are shunt fed. If arm 4 is moved a quarter wavelength at the design frequency and changed from a shunt to a series feed, the hybrid action will be maintained, although arm 4 no longer will be matched to the same Y_0. The series feed is achieved by an unbalanced-to-balanced-line transformer (*i.e.*, a balun).

A practical broad-band hybrid, shown in Fig. 3, has been designed for S band. It performs satisfactorily in a number of applications over a ± 25 per cent bandwidth centered about 3000 mc. It should be noted that this design is symmetrical about axis A–A' (Fig. 4), so that power from arms 1 or 4 will divide evenly between arms 2 and 3. It also can be seen that any power from arm 1 will arrive at the balanced-line inputs to arm 4 in phase; hence, there is isolation between arms 1 and 4. The half-wavelength sections between arms 2 or 3 and arm 4 are each divided into two quarter-wave sections having admittances Y_0 and Y_1, so that arm 4 may remain matched to Y_0. In moving arm 4 a quarter wavelength, it would become matched to Y_0/Y_1^2 if the characteristic admittance of this section of the ring were not altered.

These effects now are shown mathematically. The equivalent circuit of the hybrid is shown in Fig. 5. The admittances of the π equivalents for the transmission line sections are shown in generalized form and include the admittance of the balun to ground. This admittance is zero at the center frequency. Arm 4 is treated by introducing two nodes, 4 and 5, since it is a series feed. Power fed into arm 1 is represented by a current I_N fed to node 1. Power fed to arm 4, however, is represented schematically by a current I_N into node 4 and out of node 5, to account for the balanced push-pull feed. Assuming power is fed only to arm 1, a fifth-order system of equations is obtained:

$$\begin{bmatrix} I_N \\ 0 \\ 0 \\ 0 \\ 0 \end{bmatrix} = \begin{bmatrix} Y_{11} & Y_{12} & Y_{13} & Y_{14} & Y_{15} \\ Y_{21} & Y_{22} & Y_{23} & Y_{24} & Y_{25} \\ Y_{31} & Y_{32} & Y_{33} & Y_{34} & Y_{35} \\ Y_{41} & Y_{42} & Y_{43} & Y_{44} & Y_{45} \\ Y_{51} & Y_{52} & Y_{53} & Y_{54} & Y_{55} \end{bmatrix} \times \begin{bmatrix} V_1 \\ V_2 \\ V_3 \\ V_4 \\ V_5 \end{bmatrix}.$$

Now the following quantities can be defined:

$$Y_A = Y_{11} \qquad Y_E = Y_{35} = Y_{24} = Y_{53} = Y_{42}$$

$$Y_B = Y_{22} = Y_{33} \qquad Y_F = Y_{45} = Y_{54}$$

$$Y_C = Y_{44} = Y_{55} \qquad 0 = Y_{15} = Y_{14} = Y_{25} = Y_{34} = Y_{23}$$

$$Y_D = Y_{12} = Y_{13} = Y_{21} = Y_{31} \qquad = Y_{51} = Y_{41} = Y_{52} = Y_{43} = Y_{32}$$

(independent of frequency)

Rewriting our system of equations,

$$\begin{bmatrix} I_N \\ 0 \\ 0 \\ 0 \\ 0 \end{bmatrix} = \begin{bmatrix} Y_A & Y_D & Y_D & 0 & 0 \\ Y_D & Y_B & 0 & Y_E & 0 \\ Y_D & 0 & Y_B & 0 & Y_E \\ 0 & Y_E & 0 & Y_C & Y_F \\ 0 & 0 & Y_E & Y_F & Y_C \end{bmatrix} \times \begin{bmatrix} V_1 \\ V_2 \\ V_3 \\ V_4 \\ V_5 \end{bmatrix}. \quad (1)$$

Expanding and solving in general form,

$$V_4 = V_5 = \frac{-I_N}{D} Y_D Y_E [Y_E^2 + Y_B(Y_F - Y_C)]. \quad (2)$$

Since V_4 and V_5 are identical voltages, it can be seen that no potential difference is developed across nodes 4 and 5; hence, no power can be dissipated in arm 4 The isolation between arms 1 and 4 therefore is infinite and, since the solution is in generalized terms, independent of frequency. Solving for V_2 and V_3,

$$V_2 = V_3 = \frac{I_N Y_D}{D} [Y_F + Y_C][Y_E^2 - Y_B(Y_C - Y_F)]. \quad (3)$$

V_2 and V_3 then are equal. Arms 2 and 3, therefore, receive equal power at all frequencies. If V_1, V_2, and V_3 are specifically solved for at the center frequency, the solutions take on indeterminate forms because of the half wavelength sections of line. When evaluated, the re-

* Manuscript received by the PGMTT, December 9, 1957; revised manuscript received, May 1, 1958.

† Bogart Manufacturing Corp., Brooklyn, N. Y.
‡ Airborne Instruments Lab., Mineola, N. Y. Formerly with Bogart Manufacturing Corp., Brooklyn, N. Y.

[1] W. A. Tyrell, "Hybrid circuits for microwaves," PROC. IRE, vol. 35, pp. 1294–1306; November, 1947.

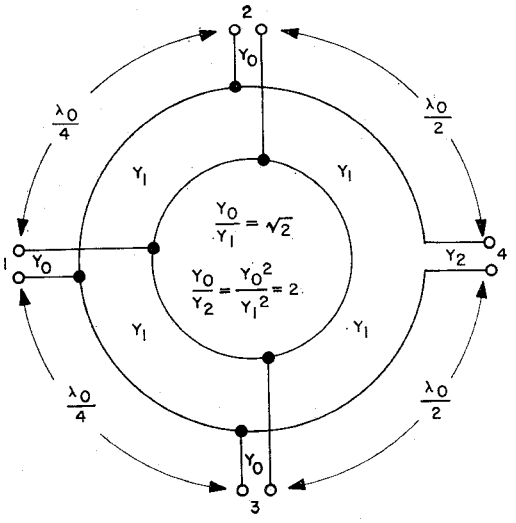

Fig. 1—Schematic representation of symmetric coaxial hybrid ring.

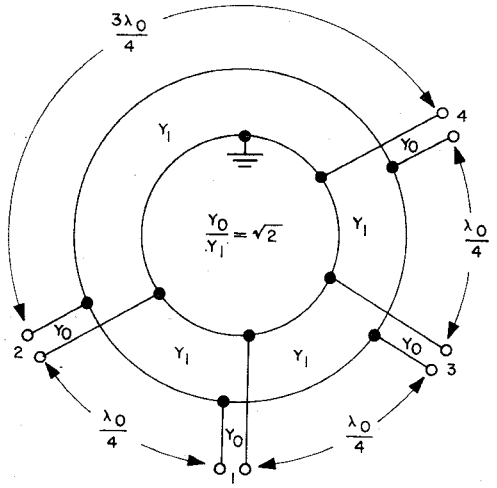

Fig. 2—Schematic representation of conventional 6/4λ hybrid ring.

sults are identical with those for the conventional hybrid,

$$V_1 = \frac{I_N}{2\sqrt{2}}, \qquad V_2 = V_3 = -j\frac{I_N}{4}. \tag{4}$$

Consider now the hybrid behavior if power is fed to arm 4 instead of to arm 1. The current matrix becomes

$$\begin{bmatrix} 0 \\ 0 \\ 0 \\ I_N \\ -I_N \end{bmatrix}.$$

Although infinite isolation has been proved, it can be shown that, for this case, $V_1 = 0$. V_2 and V_3 may be solved for

$$V_2 = -V_3 = \frac{I_N Y_E}{D}\left[Y_A Y_E^2 + (Y_C + Y_F)(2Y_D^2 - Y_A Y_B)\right]. \tag{5}$$

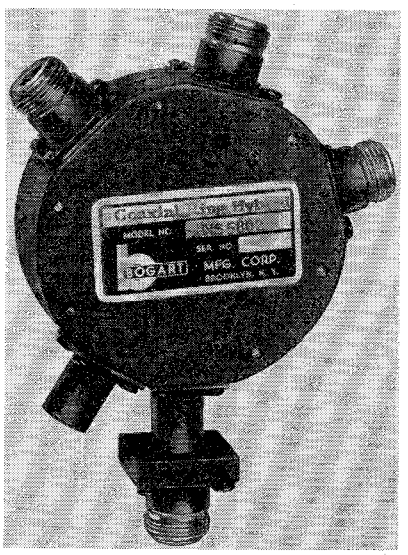

Fig. 3—Symmetric coaxial hybrid ring

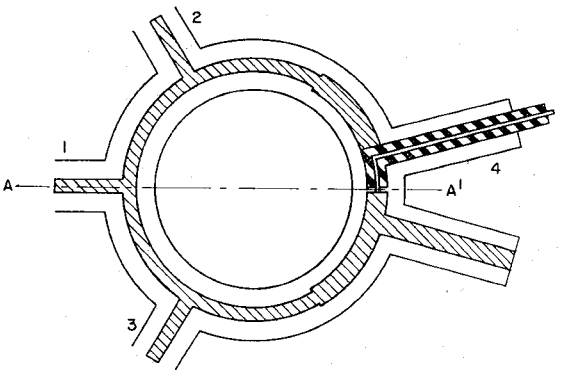

Fig. 4—Cross section of symmetric coaxial hybrid ring.

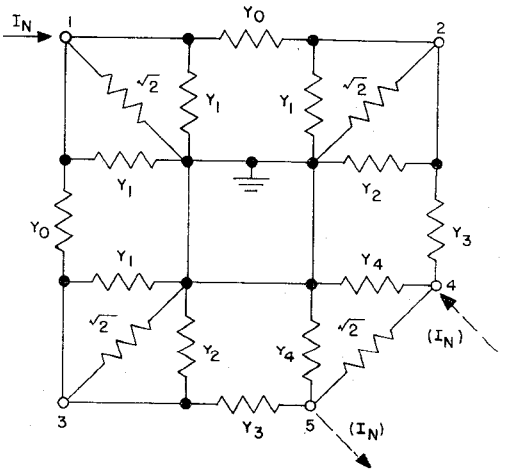

Fig. 5—Equivalent circuit of symmetric coaxial hybrid ring.

For the case of power being fed to arm 4, arms 2 and 3 will receive signals which are equal but out of phase, and again independent of frequency.

It is of interest to determine the isolation between arms 2 and 3. If a current I_N was fed to node 2, for example, V_2 and V_3 could be solved for, and their

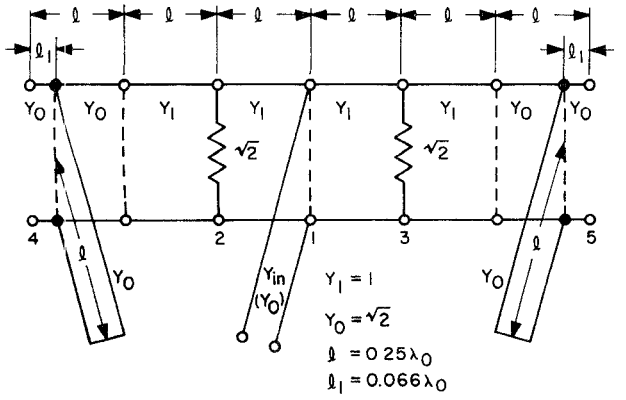

Fig. 6—Equivalent circuit of symmetric coaxial hybrid ring, bisected at arm 1.

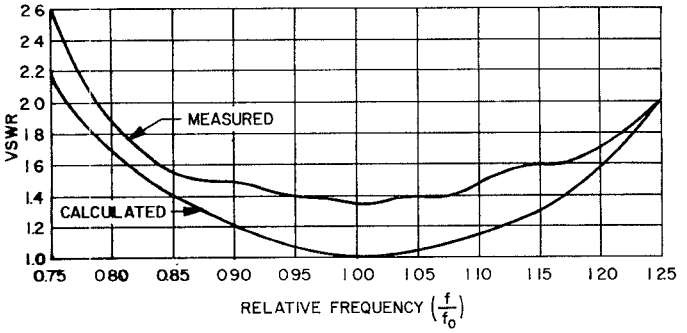

Fig. 7—VSWR vs frequency at arm 1 of symmetric hybrid ring.

ratio evaluated as isolation. At the center frequency, $V_3 = 0$, so that the isolation is infinite. Since there is a lack of symmetry about arms 2 and 3, the isolation is not independent of frequency. At the ends of a ± 25 per cent band, it has been evaluated at approximately 13.5 db.

The VSWR at arms 1 and 4 can be calculated by evaluating V_1 and $V_4 - V_5$, respectively, with power fed into these arms. The calculations, however, may be greatly simplified by employing the symmetry conditions. To find input admittance and VSWR at arm 1, bisect the hybrid through axis A–A' (Fig. 4) and unfold it into the form seen in Fig. 6. Admittances looking left and right are identical; it is necessary to compute only the admittance looking in one direction, and then double it to obtain total admittance. The use of a Smith Chart greatly facilitates the calculations. Y_{in} (normalized to Y_0) equals unity at the design frequency, f_0, assuming all other arms are terminated in Y_0. Therefore, VSWR is also unity. VSWR values, computed by this technique, are plotted as a function of fractional bandwidth in Fig. 7.

To find input admittance or VSWR at arm 4, the ring may be bisected again through axis A–A' and unfolded into the form shown in Fig. 8. Using the Smith Chart, the input VSWR values at arm 4 have been computed and are shown in Fig. 9.

The characteristics of the symmetric hybrid have been measured at S band and, for comparison, have

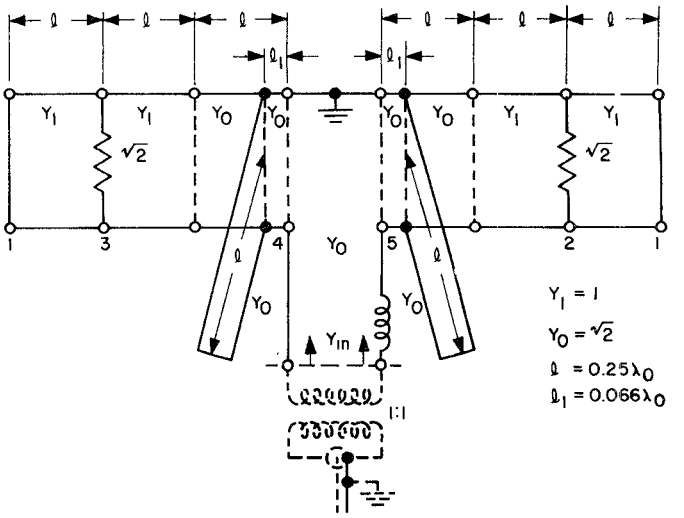

Fig. 8—Equivalent circuit of symmetric coaxial hybrid ring, bisected at arm 4.

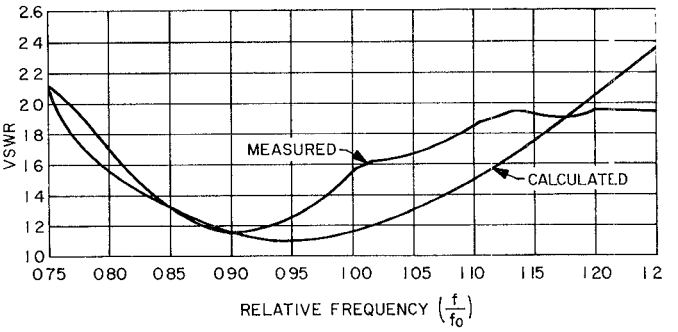

Fig. 9—VSWR vs frequency at arm 4 of symmetric hybrid ring.

been plotted in terms of fractional bandwidth. The results represent average data measured on 15 production units. Input VSWR's at arms 1 and 4 have been plotted on Figs. 7 and 9, respectively. The measured isolations between arms 1 and 4 and between arms 2 and 3 are shown in Figs. 10 and 11, respectively. Minimum measured isolation between arms 1 and 4 was in excess of 38 db. The jagged nature of the curve is caused by the imperfections in the matched loads terminating the output arms during measurement, and also by the residual unbalances in the reflections created in the tee junctions and connectors of these arms. When dealing with isolations of the magnitude measured here, even a very small reflection at one of the output arms has a marked effect on the isolation reading.

The power unbalance at the various arms also has been measured and is shown in Figs. 12 and 13. In no case does the unbalance in output power at arms 2 and 3 exceed 0.1 db, with signal input at either arm 1 or arm 4.

Additional Considerations

The sections of transmission line between arm 4 and arms 2 and 3 are not absolutely necessary for the electrical operation of the hybrid. If another method, such

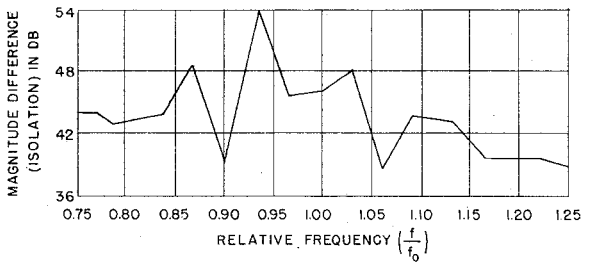

Fig. 10—Measured isolation between arms 1 and 4 of symmetric hybrid ring.

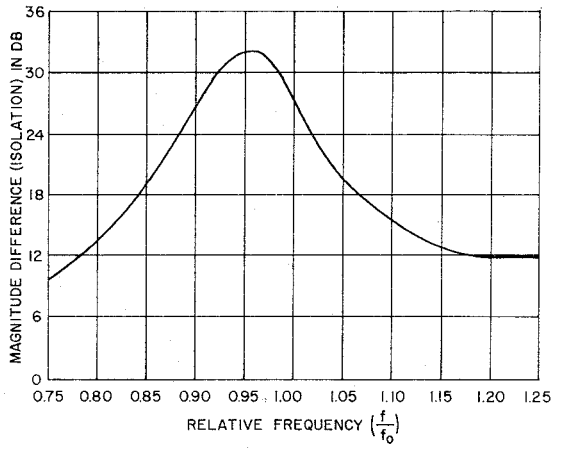

Fig. 11—Measured isolation between arms 2 and 3 of symmetric hybrid ring.

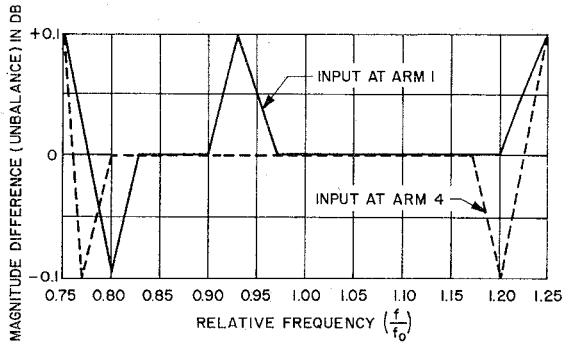

Fig. 12—Measured relative magnitude (unbalance) of output at arms 2 and 3 of symmetric hybrid ring, with signal input at arm 1 and at arm 4.

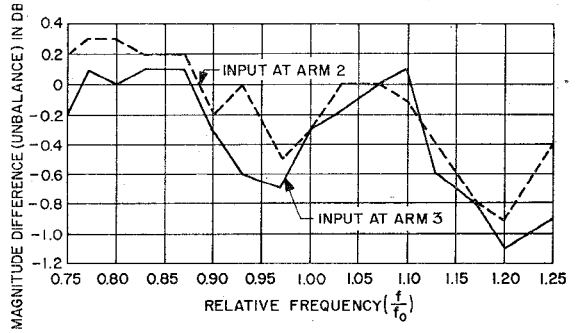

Fig. 13—Measured relative magnitude (unbalance) of output at arms 1 and 4 of symmetric hybrid ring, with signal input at arm 2 and at arm 3.

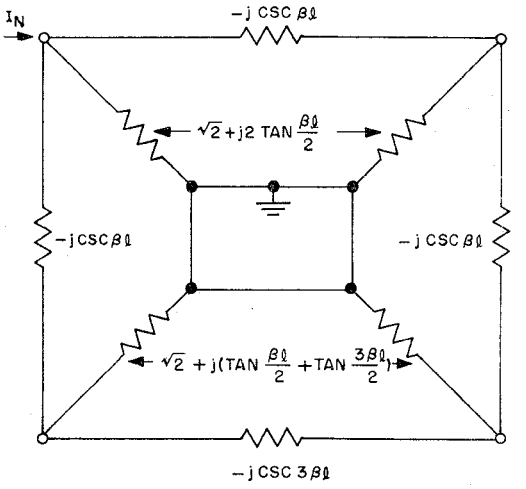

Fig. 14—Equivalent circuit of conventional 6/4λ hybrid ring; admittances normalized to Y_1.

as a quarter-wave transformer within the arm itself, is employed for matching arm 4, and the mechanical arrangement of coaxial inputs is altered, these two sections of line may be eliminated. The broad-band performance will be somewhat improved. Such a design is particularly adaptable to the lower frequency bands, but fabrication is extremely difficult at frequencies above S band.

Conventional Coaxial Hybrid Ring

A conventional coaxial hybrid ring (Fig. 2) suffers from several shortcomings in broad-band applications. For example, ifthe hybrid is to be used with a balanced mixer, the isolation between the signal and local oscillator arms (1 and 4, respectively) will fall off sharply as the frequency is varied from design center. The balance between the signals reaching the two output arms (2 and 3) also will deteriorate with frequency change.

The conventional hybrid is shown in Fig. 14 as an equivalent lumped-parameter network. Assuming a constant current I_N applied to node 1, the matrix equation may be written

$$\begin{bmatrix} I_N \\ 0 \\ 0 \\ 0 \end{bmatrix} = \begin{bmatrix} Y_{11} & Y_{12} & Y_{13} & Y_{14} \\ Y_{21} & Y_{22} & Y_{23} & Y_{24} \\ Y_{31} & Y_{32} & Y_{33} & Y_{34} \\ Y_{41} & Y_{42} & Y_{43} & Y_{44} \end{bmatrix} \times \begin{bmatrix} V_1 \\ V_2 \\ V_3 \\ V_4 \end{bmatrix}.$$

The nodal voltages are evaluated at f_0 as

$$V_1 = \frac{I_N}{2\sqrt{2}}; \quad V_2 = V_3 = -j\frac{I_N}{4}; \quad V_4 = 0. \tag{6}$$

If we assume a constant current applied to node 4, the current matrix becomes

$$\begin{bmatrix} 0 \\ 0 \\ 0 \\ I_N \end{bmatrix}.$$

The nodal voltages at f_0 are evaluated again.

$$V_2 = -j\frac{I_N}{4}; \quad V_3 = +j\frac{I_N}{4}; \quad V_4 = \frac{I_N}{2\sqrt{2}}; \quad V_1 = 0. \quad (7)$$

The voltages have the same form as in (6) with the exception that V_2 and V_3 are 180 degrees out of phase. Then, it may be concluded that, at f_0, there is infinite isolation between arms 1 and 4, and power is divided equally between arms 2 and 3.

This technique can be used to calculate the behavior of the hybrid over a frequency band. The results have been computed over a large bandwidth and are compared with available measured data in Figs. 15–17.[2] It is seen that isolation and balance deteriorate rapidly when the frequency departs from f_0.

Conclusion

In the case of the symmetric hybrid, correlation between the calculated and experimental data is close. Deviations in VSWR can be attributed to the inherent mismatch of the Type N connectors and the tee junctions.

It has been mentioned that even slight residual reflections from the output arms might cause radical changes in the apparent isolation between arms 1 and 4. This is largely dependent on the relative phase of the reflections and, for lower values of isolation (less than 30 db), the effect is much less noticeable. This explains the jagged nature of the curve in Fig. 10, whereas Fig. 11 shows a smooth curve.

Maximum measured isolation between arms 2 and 3 of the symmetric hybrid is lower than that of the conventional design. This might be attributed to the disturbing effects of the baluns and the physical structure of arm 4. In many applications, however, the isolation between arms 2 and 3 is relatively unimportant.

Bibliography

[1] W. V. Tyminski and A. E. Hylas, "A wide-band hybrid ring for UHF," Proc. IRE, vol. 41, pp. 81–87; January, 1953.
[2] T. Morita and L. S. Sheingold, "A coaxial magic T," IRE Trans. on Microwave Theory and Techniques, vol. MTT-1, pp. 17–23; November, 1953.
[3] J. Reed and G. J. Wheeler, "A method of analysis of symmetrical four-port networks," IRE Trans. on Microwave Theory and Techniques, vol. MTT-4, pp. 246–252; October, 1956.
[4] R. V. Pound, "Microwave-Mixers," M.I.T. Rad. Lab. Ser., McGraw-Hill Book Co., Inc., New York, N. Y., vol. 16, p. 268; 1948.

[2] J. E. Butler, "Design of strip transmission line systems and antennas," thesis submitted in partial fulfillment of requirements for the M.S.E.E. degree, U. S. Naval Postgraduate School, Monterey, Calif.; June, 1955. Experimental work performed at Airborne Instruments Lab., Inc., Mineola, N. Y.

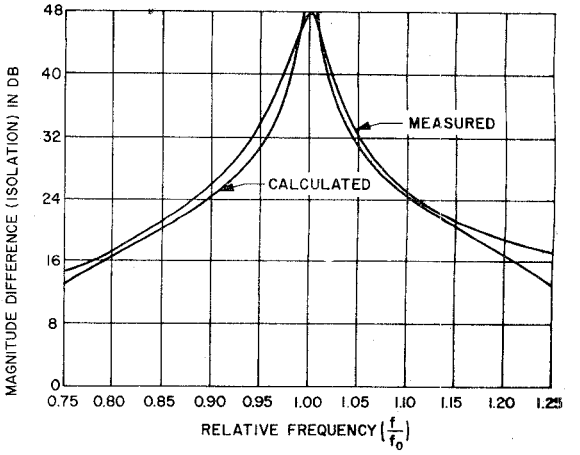

Fig. 15—Isolation between arms 1 and 4 or between arms 2 and 3 of conventional hybrid ring.

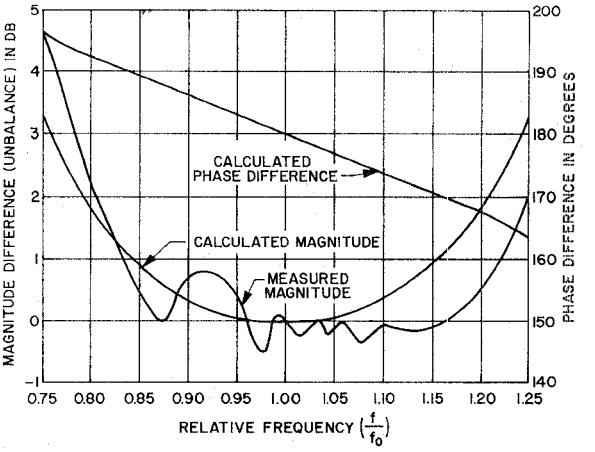

Fig. 16—Relative phase and magnitude (unbalance) of output at arms 2 and 3 of conventional hybrid ring, with signal input at arm 4.

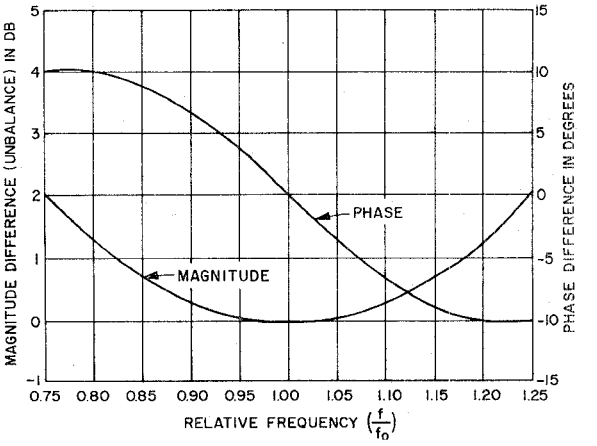

Fig. 17—Calculated relative phase and magnitude (unbalance) of output at arms 2 and 3 of conventional hybrid ring, with signal input at arm 1.